Ore Geology Reviews 133 (2021) 104129

Contents lists available at ScienceDirect

Ore Geology Reviews

journal homepage: www.elsevier.com/locate/oregeorev

Reassessment of thermal preservation of organic matter in the Paleoproterozoic McArthur River (HYC) Zn-Pb ore deposit, Australia

Galina Vinnichenko [a,*], Janet M. Hope [a], Amber J.M. Jarrett [b], Neil Williams [a], Jochen J. Brocks [a,*]

[a] Research School of Earth Sciences, The Australian National University, Canberra, Australian Capital Territory 2601, Australia
[b] Geoscience Australia, Canberra, Australian Capital Territory 2601, Australia

ARTICLE INFO

Keywords:
Barney Creek Formation
Biomarkers
McArthur Basin
polycyclic aromatic hydrocarbons (PAH)
Rock-Eval

ABSTRACT

The 1.64 Ga old McArthur River (HYC) Zn-Pb deposit in northern Australia is one of the best preserved clastic-dominated, stratiform base-metal deposits. However, the mechanisms of ore formation are still controversial. To characterize the influence of metal-bearing fluids on organic matter in the McArthur River mine, we used lipid biomarkers in combination with compound-specific isotope analysis and Rock-Eval pyrolysis on a succession covering the hanging wall, orebody, inter-ore layers and foot wall. Aromatic and methyldiamantane maturity parameters indicate that bitumens through the entire succession, including the ore zone, fall into the beginning of the gas window (~160 °C). The thermal maturity of kerogen in the hanging and foot wall is consistent with this degree of thermal alteration. By contrast, kerogen in the ore zone possesses extremely high thermal maturities that are inconsistent with the bitumen. This temperature anomaly shows that the extractable hydrocarbons migrated into the orebody after mineralization, most probably from surrounding sediments of the Barney Creek Formation. Polycyclic aromatic hydrocarbons (PAH) found in the McArthur River orebody are detected in similar distributions in the unmineralized hanging wall and foot wall and are thus not the products of hydrothermal activity, as previously assumed, but formed through burial-temperature processes. Therefore, the hydrocarbons in the McArthur River ore zone do not yield information about the temperature of mineralizing fluids, negating earlier suggestions for temperatures of 200 °C, or 250 to 400 °C. Yet, based on kerogen maturity, the organic matter in ore lenses and inter-ore breccias is still severely altered. The data is most consistent with the flow of metal-bearing fluids with temperatures in the range of thermochemical sulphate reduction but inconsistent with the activity of bacterial sulphate reducers.

1. Introduction

The McArthur River (or HYC) clastic-dominated (CD) stratiform Zn-Pb deposit in northern Australia is one of the least altered CD Zn-Pb deposits yet discovered. Even though the deposit is 1.64 Ga old, primary-forming features are well preserved (Eldridge et al., 1993; Ireland et al., 2004), and McArthur River deposit is therefore well suited for ore genesis investigations on the economically important CD-type of Zn-Pb mineralization. Although much research has been carried out to understand the McArthur River ore-forming processes, the precise mechanisms are still a topic of debate.

Two contrasting groups of ore-forming models have been proposed for the McArthur River deposit. The first are the relatively low temperature syngenetic synsedimentary models (Ireland et al., 2004; Large et al., 2002, 1998, 2001; McGoldrick et al., 2010), the most comprehensive of which is the brine-pool model of Ireland et al. (2004) where the three main sulphide minerals, pyrite, sphalerite and galena form from exhaled mineralizing fluids which pond in a brine pool. Sulphide precipitation in this model takes place mostly in response to bacterial sulphate reduction. The second are the much hotter post-sedimentary diagenetic to epigenetic models (Chen et al., 2003; Eldridge et al., 1993; Logan et al., 2001; Magnall et al., 2020; Spinks et al., 2020; Symons, 2007; Williford et al., 2011). The most detailed of these, initially developed by Eldridge et al. (1993) and subsequently refined by Logan et al. (2001) and Chen et al. (2003), involves the early diagenetic formation of pyrite by bacterial sulphate reduction in carbonaceous sediments and the later introduction of hot Zn- and Pb-rich fluids into the sediments from nearby faults. Ore formation is postulated to have

* Corresponding authors.
E-mail addresses: galina.vinnichenko@anu.edu.au (G. Vinnichenko), jochen.brocks@anu.edu.au (J.J. Brocks).

https://doi.org/10.1016/j.oregeorev.2021.104129
Received 14 October 2020; Received in revised form 1 March 2021; Accepted 13 March 2021
Available online 19 March 2021

occurred meters to tens of meters beneath the sediment–water interface by way of sulphate reduction. However, Logan et al. (2001) were ambivalent whether the reduction was bacterial or thermochemical. Subsequently Chen et al. (2003) proposed fluid temperatures of 250–400 °C, a range favouring thermochemical sulphate reduction, but also raising the possibility that the reduced sulphide sulphur may have been carried in by the mineralizing fluids, as initially suggested by Eldridge et al. (1993). A better understanding of the ore-forming fluids temperature is pivotal to determining the actual McArthur River processes.

The McArthur River orebody is hosted in the 1.64 Ga Paleoproterozoic Barney Creek Formation (Fm), which also contains dubious microfossils (Crick, 1992; Oehler, 1977) and biomarkers of Proterozoic age (Brocks et al., 2005; Brocks and Schaeffer, 2008; Summons et al., 1988). Previous studies on the McArthur River organic matter applied biomarker distributions and maturity indices to estimate the temperature of the ore-forming fluids (Logan et al., 2001; Chen et al., 2003; Williford et al., 2011). The suggested temperatures of 200–250 °C (Williford et al. 2011) or even 250–400 °C (Chen et al. 2003) were used to support an epigenetic model involving basin-derived hot mineralizing fluids. However, some of the previous biomarker studies were affected by contamination, based on the presence of diagnostic Phanerozoic sterane signals (e.g., Logan et al., 2001). Studies by Chen et al. (2003) and Williford et al. (2011) investigated samples along the horizontal trajectory of expected brine flow in individual ore bodies. The organic geochemistry of the McArthur River deposit was reviewed by Greenwood et al. (2013).

The current study provides the first hydrocarbon analysis of the full succession that harbours the McArthur River ore deposit, including the hanging wall, orebody, inter-ore layers and foot wall. The goal of this research is to compare organic matter in mineralized and unmineralized zones of the McArthur River mine using lipid hydrocarbons in combination with Rock-Eval pyrolysis and compound-specific isotope analysis, and to determine the impact the mineralizing fluids had on the organic geochemistry of the Barney Creek Fm.

2. Geological setting and samples

The McArthur River mine is located in the northern Australian McArthur Basin close to the Emu Fault. The Paleoproterozoic–Mesoproterozoic McArthur Basin contains predominantly shallow marine siliciclastic and carbonate succession that is subdivided into the Tawallah, McArthur, Nathan and Roper groups in the southern part of the basin (Fig. 1) (Ahmad et al., 2013; Jackson et al., 1987; Munson, 2014). The McArthur Group (~1690 to ~ 1614 Ma) is represented by shallow to deep marine carbonates, shales and sandstones (Jackson et al., 1987; Kunzmann et al., 2019), deposited during predominant basin subsidence with occasional extensional and compressional periods (Blaikie and Kunzmann, 2020). The 1640 ± 4 Ma Barney Creek Fm of the McArthur Group occurs conformably between the Teena Dolostone (below) and the Reward Dolostone (above) and comprises laminated dolomitic, carbonaceous and pyritic siltstone and shale (Jackson et al., 1987; Page and Sweet, 1998). The Barney Creek Fm, which was deposited in a quiet, anoxic, sub-wave-base environment, records two maximum flooding surfaces and, together with the overlying Reward Dolostone, includes two transgressive–regressive sequences (Bull, 1998; Kunzmann et al., 2019). Jackson et al. (1987) subdivided the Barney Creek Fm into three members, from bottom to top the Cooley Dolostone, W-Fold Shale and HYC Pyritic Shale. Outside of the McArthur River mine, these three members are overlain by a thick, undifferentiated

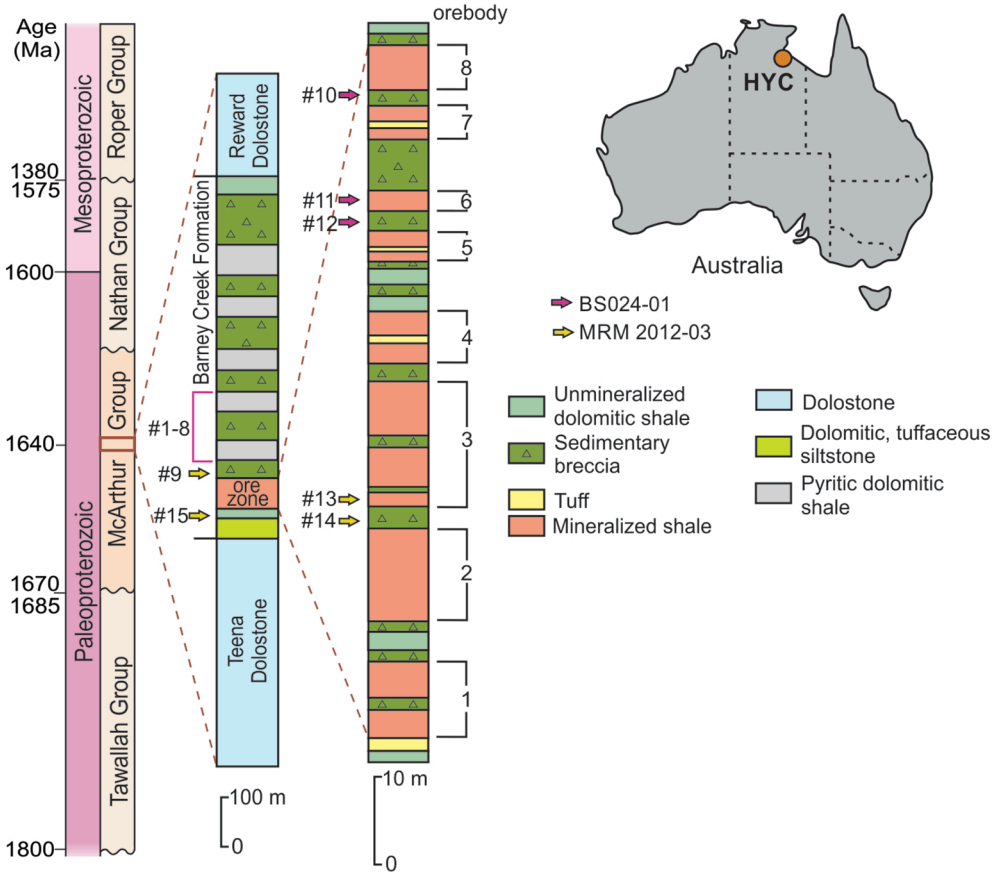

Fig. 1. Simplified stratigraphy of the southern McArthur Basin and expanded McArthur River ore zone section (after Large et al., 1998) showing fifteen sampled intervals in two drill cores, BS042-01 and MRM 2012–03.

upper section that is not preserved in the HYC sub-basin (Kunzmann et al., 2019). The orebody is located within the HYC Pyritic Shale Member and consists of eight stacked ore lenses with average thicknesses ranging from ~2 to ~14 m, separated by unmineralized pyritic dolomitic shale or dolomitic breccia (Fig. 1) (Eldridge et al., 1993). Sulphide mineralization occurs as mainly fine-grained bands and crystals of predominantly pyrite, galena and sphalerite, along with minor arsenopyrite and chalcopyrite (Ireland et al., 2004; Spinks et al., 2020).

In the current study, fifteen samples (Fig. 1, Table 1) were collected for organic geochemical analysis from the hanging wall, inter-ore, orebody and foot wall of two drill cores from the McArthur River Mine (MRM 2012-03 and BS024-01). Nine hanging wall samples as well as one foot wall sample consisted of unmineralized black shale, dolomitic siltstone and shale, pyritic shale and nodular dolomite (Table 1). Ore zone samples were represented by two mineralized shales, two inter-ore breccias and one nodular dolomite (Table 1). For comparison, we further included one low maturity unmineralized Barney Creek Fm sample (#16) from the LV09 drill core distal to the mine (Table 1).

3. Methods

3.1. Biomarker analysis

Since drilling fluids or other anthropogenic petroleum products can significantly compromise the results of biomarker analysis on Precambrian rocks, it is crucial to recognize and remove contaminants using exterior/interior experiments (Brocks et al., 2008) and only interpret demonstrably indigenous molecular fossils from McArthur River samples. Biomarker analysis was performed at the Australian National University and followed protocols and methods described in detail elsewhere (e.g., Brocks et al., 2008; Jarrett et al., 2013; Vinnichenko et al., 2020). First of all, ~3 mm were removed from the exterior of all drill core specimens using a solvent-cleaned precision diamond wafering saw (Buehler IsoMet 1000) or a wet table saw (Nortel Machinery Inc.), depending on sample size and shape. Then a clean Rocklabs iron puck mill was used to ground the exterior (E) and interior (I) rock portions to a < 240-mesh powder. Later, E and I rock powders were extracted with a Dionex Accelerated Solvent Extractor (ASE 200) using 90% DCM and 10% methanol. Prior fractionation, extracts were filtrated over freshly precipitated elemental copper to remove elemental sulphur. All extracted bitumens were separated into saturated, aromatic, and polar fractions with microcolumn (pasteur pipette) chromatography over annealed and dry-packed silica gel (7 cm) using 1.5 ml of *n*-hexane, 4 ml of *n*-hexane:DCM (1:1, v/v) and 3 ml of DCM:methanol (1:1, v/v) respectively. Gas chromatography–mass spectrometry (GC–MS) analyses were carried out on an Agilent 6890 GC coupled to a Micromass Autospec Premier double sector MS. The GC was equipped with a 60 m DB-5MS capillary column (0.25 mm ID, 0.25 μm; Agilent) and used helium as the carrier gas at a constant flow rate of 1 ml min^{-1}. Full Scan analyses were performed for saturated and aromatic fractions. Laboratory contaminants remained below detection limits in the cumulative system blanks that experienced the whole sequence of procedures along with samples.

Table 1
McArthur River sample information and biomarker maturity parameters.

Sequence	Sample ID	Internal sample ID	Drill core	Depth, (m)	Relative depth[a], (m)	Sample description	MPI[b]	Rc (MPI)[c]	MPDF[d]	Rc (MPDF)[e]	MPR[f]	Rc (MPR)[g]	MDI[h](%)
Hanging wall	#1	17G013	BS024-01	16.4	−182.6	Massive black shale	1.30	1.18	0.63	1.24	1.88	1.21	32
	#2	17G019	BS024-01	41.5	−157.7	Laminated black shale	1.40	1.24	0.65	1.30	2.19	1.28	30
	#3	19G019	BS024-01	63.5	−135.6	Dolomitic siltstone	1.26	1.16	0.61	1.20	1.86	1.21	37
	#4	19G020	BS024-01	85.7	−113.4	Dolomitic siltstone	1.29	1.17	0.62	1.22	1.95	1.23	39
	#5	17G020	BS024-01	105.1	−94.1	Pyritic shale	1.19	1.11	0.57	1.10	1.46	1.10	37
	#6	17G021	BS024-01	146.1	−53.1	Dolomitic siltstone	1.47	1.28	0.70	1.40	2.74	1.37	n.d.
	#7	19G023	BS024-01	167.5	−31.5	Dolomitic siltstone	1.24	1.14	0.69	1.37	2.77	1.38	n.d.
	#8	19G021	BS024-01	191.1	−7.9	Pyritic shale	1.44	1.26	0.68	1.36	2.58	1.35	37
	#9	17G011	MRM 2012–03	157.8	−3.0	Fine scale nodular dolomite	1.29	1.17	0.62	1.22	1.99	1.24	37
Interore 7/8	#10	17G018	BS024-01	201.1	2.1	Interore breccia	1.47	1.28	0.66	1.32	2.45	1.32	33
Orebody 6	#11	17G016	BS024-01	210.0	11.0	Mineralized shale	1.55	1.33	0.68	1.35	2.57	1.35	n.d.
Interore 5/6	#12	17G017	BS024-01	215.7	16.7	Interore breccia	1.44	1.27	0.70	1.40	2.83	1.39	32
Lower 3rd orebody	#13	17G014	MRM 2012–03	190.4	29.5	Mineralized shale	1.28	1.17	0.64	1.26	2.13	1.26	33
Interore 2/3	#14	17G015	MRM 2012–03	197.9	37.0	Nodular dolomite	1.22	1.13	0.59	1.16	1.71	1.17	41
Foot wall	#15	17G012	MRM 2012–03	210.8	49.9	Dolomitic shale	1.32	1.19	0.62	1.22	1.92	1.22	36
Unmineralized BCF	#16	17G008	LV09	477	–	Dolomitic siltstone	0.64	0.79	0.39	0.71	0.81	0.85	–

[a] Depth in meters relative to the top of the ore body. [b]Methylphenanthrene index MPI-1 = 1.5*(2-MP + 3-MP)/(P + 1-MP + 9-MP), where P = phenanthrene, MP = methylphenanthrene (Radke and Welte, 1983). [c]Calculated vitrinite reflectance Rc(MPI-1) = 0.6*MPI-1 + 0.4 for absence of the MPI-1 reversal (Radke and Welte, 1983). [d]Methylphenanthrene distribution factor MPDF = (3-MP + 2-MP)/(3-MP + 2-MP + 9-MP + 1-MP) (Kvalheim et al., 1987). [e]Calculated vitrinite reflectance Rc (MPDF) = 2.242*MPDF − 0.166 (Kvalheim et al., 1987). [f]Methylphenanthrene ratio MPR = 2-MP/1-MP (Radke, 1988). [g]Calculated vitrinite reflectance Rc(MPR) = 1.1*$\log_{10}$(MPR) + 0.95 (Radke, 1988). [h]Methyldiamantane index MDI = 4-MD/(1-MD + 3-MD + 4-MD), where MD = methyldiamantane (Chen et al., 1996). n.d. – not detected.

3.2. Isolation of kerogen

Kerogen isolation for McArthur River samples was undertaken at Geoscience Australia following the in-house protocol. The analysis was performed on 10–11 g rock powder that had already undergone solvent extraction with ASE 200. Decarbonation of extracted powders was achieved using 15% hydrochloric acid (HCl), with samples then centrifuged 3 times with deionised water (2000 rpm for 5 min) for neutralising the HCl. 48% Hydrofluoric acid (HF) was used to remove silicate minerals. Samples were mixed with 100 ml of deionised water and 100 ml of HF and further stirred at room temperature on an agitator plate (150 rpm for 7 h). The mixture was then allowed to stand for 6 h, the dilute HF solution decanted, and fresh solution (50 ml of water and 50 ml of HF) added. The stirring procedure was repeated and 20 ml of warm (50 °C) saturated boric acid (H_3BO_3) solution was added to each sample, which was still immersed in HF solution. After the stirring procedure was repeated and samples were settled for 6 h, the dilute HF/boric acid solution was siphoned off. Samples were washed with warm (50 °C) deionised water 4 times using centrifugation (2000 rpm for 5 min). Treatment with 15 ml of 15% HCl in a water bath set to 65 °C for 2 h was used as an additional step to remove carbonates. To neutralise the HCl, samples were centrifuged with warm deionised water 3 times. For removal of heavy minerals, 20 ml of sodium polytungstate solution was added to each sample, mixed well and centrifuged. The floats and sinks were collected into separate test tubes and washed with warm deionised water. The kerogen concentrate was dried in an oven at 45 °C.

3.3. Rock-Eval pyrolysis

Total organic carbon (TOC) content and hydrocarbon potential were measured using a Rock-Eval 6 Turbo™ (Vinci Technologies, France) at Geoscience Australia and Moscow State University following the methodology, described in Jarrett et al. (2018). The analyses were performed on 60 mg of bulk rock powder or 3 mg of concentrated kerogen. The initial pyrolysis oven temperature was set at 300 °C (held for 5 min) and then ramped to 650 °C with 25 °C per minute rate. The oxidation oven was held at 400 °C for 3 min followed by ramping to 850 °C at 20 °C per minute, with a final hold time of 5 min. The flame ionisation detector (FID) was calibrated by running the standard 'IFP 160000′. For each batch of samples, the analysis blanks were run and later automatically subtracted from sample data.

The main parameters obtained with this method are S1 (free hydrocarbons), S2 (hydrocarbon potential), S3 (CO_2 potential), Tmax (the pyrolysis temperature at the S2 peak maximum) and TOC (total organic carbon). Other parameters are defined in Table 3.

3.4. Stable hydrogen and carbon isotopes

Stable hydrogen and carbon isotopic compositions of *n*-alkanes were analysed as duplicates using gas chromatography-isotopic ratio mass spectroscopy (GC-IRMS) at Geoscience Australia. Prior to isotope analyses, *n*-alkanes were separated from the saturated fraction using 0.5 mg of 5 Å zeolite molecular sieve (Grace Davison) in cyclohexane. The sieve was digested in HF (32%, 3 ml) to release the *n*-alkanes, which further were extracted with 3 ml *n*-hexane. All $\delta^{13}C$ and $\delta^{2}H$ values are reported in permil (‰) notation relative to VPDB and VSMOW respectively. Average standard deviation of individual compounds is 0.13‰ for $\delta^{13}C$ and 2‰ for $\delta^{2}H$. Organic carbon isotope analyses of kerogen ($\delta^{13}C_{ker}$) was measured with Sercon 20–20 combustion IRMS.

4. Results

4.1. Biomarker distributions and thermal maturity

Extracted Barney Creek Fm bitumens from fifteen mine samples illustrate typical mid-Proterozoic hydrocarbon distributions with large unresolved complex mixture and high methyl-alkane/*n*-alkane ratios (Pawlowska et al., 2013). Fig. 2 compares the total ion chromatograms of the saturated and aromatic fractions of a hanging wall and orebody sample. Saturated fractions contain unimodal distribution of *n*-alkanes ranging from C_{11} to C_{30} with a maximum at C_{13} to C_{17} (Fig. 2a, b). The total ion chromatograms of the McArthur River aromatic fractions indicate the presence of polycyclic aromatic hydrocarbons (PAH) such as phenanthrene, pyrene, chrysene, benzo[e]pyrene, benzo[ghi]perylene and coronene in the ore zone as well as in the hanging wall (Fig. 2c, d). Interestingly, even higher abundances of PAH (relative to TOC) were detected in low maturity (Rc = 0.7–0.8%) unmineralized Barney Creek Fm sediments from the LV09 drill hole, which is located 40 km south of the McArthur River mine (Table 2).

The maturity level of all McArthur River samples was too high for preservation of polycyclic biomarkers such as hopanes or steranes. However, the McArthur River extracts contain diamondoids and phenanthrenes that can be used as maturity parameters. These compounds occur as various structural isomers with different thermal stabilities. Under thermal stress, the concentration of more stable isomers rises relative to less stable configurations (e.g., Greenwood et al., 2013). The relative abundances of these molecules may thus serve as thermal maturity indicators. Common hydrocarbon-based maturity indices, defined in Table 1, include the methyl diamantane index (MDI; Chen et al., 1996), methyl-phenanthrene index (MPI; Radke and Welte, 1983), methyl-phenanthrene distribution factor (MPDF; Kvalheim et al., 1987) and methyl-phenanthrene ratio (MPR; Radke, 1988). For sedimentary rock specimens of the Phanerozoic eon, vitrinite reflectance measurements (%Ro) represent a standard method to estimate thermal maturity of solid organic matter. Since vitrinite, an organic maceral deriving from plants, did not exist in the Proterozoic, hydrocarbon parameters such as MDI, MPI, MPDF and MPR can be re-calculated to yield vitrinite reflectance equivalent values (Rc, where 'c' stands for calculated), making comparison of different maturity parameters more easy (formulas are provided in Table 1). Rc values between 0.6 and 1.2% correspond to thermally mature organic matter in the oil window zone, while values >1.2% denote overmature stage or gas window zone (Baskin, 1997).

Table 1 summarises the hydrocarbon-based maturity indices MDI, MPI, MPDF and MPR for McArthur River samples. MDI range from 30 to 41% and correspond to Rc values between 1.1 and 1.3% (Chen et al., 1996), while Rc based on MPDF and MPR fall into the range 1.1–1.4% for the entire sediment package (Table 1, Fig. 3b). Generally, MPI values rise with increasing maturity, but above a certain threshold (Rc = 1.7%), MPI values start to decrease again (Boreham et al., 1988). Such a reversal can be recognized by phenanthrene/methyl-phenanthrene (P/MP) ratios > 1 (Brocks et al., 2003). The Rc(MPI) further must be calculated using two different formulas depending on presence or absence of the reversal (Radke and Welte, 1983). Since P/MP ratios for the McArthur River samples vary from 0.3 to 0.5, the MPI is not reversed and the corresponding Rc(MPI) values fall into the range between 1.1 and 1.3%, consistent with other maturity parameters (Rc from MDI, MPDF and MPR). Orebody samples from this study show slightly higher maturity levels in comparison with previously published bitumens for the ore lens 5 that yielded Rc(MPDF) = 0.9–1.1% and Rc(MPR) = 0.9–1.0% (calculated from Table 1 in Williford et al. 2011). Although Williford et al. (2011) reported Rc(MPI) values up to 1.6%, the P/MP ratios in their study varied from 0.1 to 0.2, indicating that MPI reversal did not occur. Therefore, after applying the correct formula for absence of the reversal, Rc(MPI) in Williford et al. (2011) should range between 1.1 and 1.2%, consistent with Rc(MPDF) and Rc(MPR) values from their study.

4.2. Rock-Eval data

The results of Rock-Eval pyrolysis on bulk rock and kerogen concentrates of eleven samples are represented in Table 3. The majority of

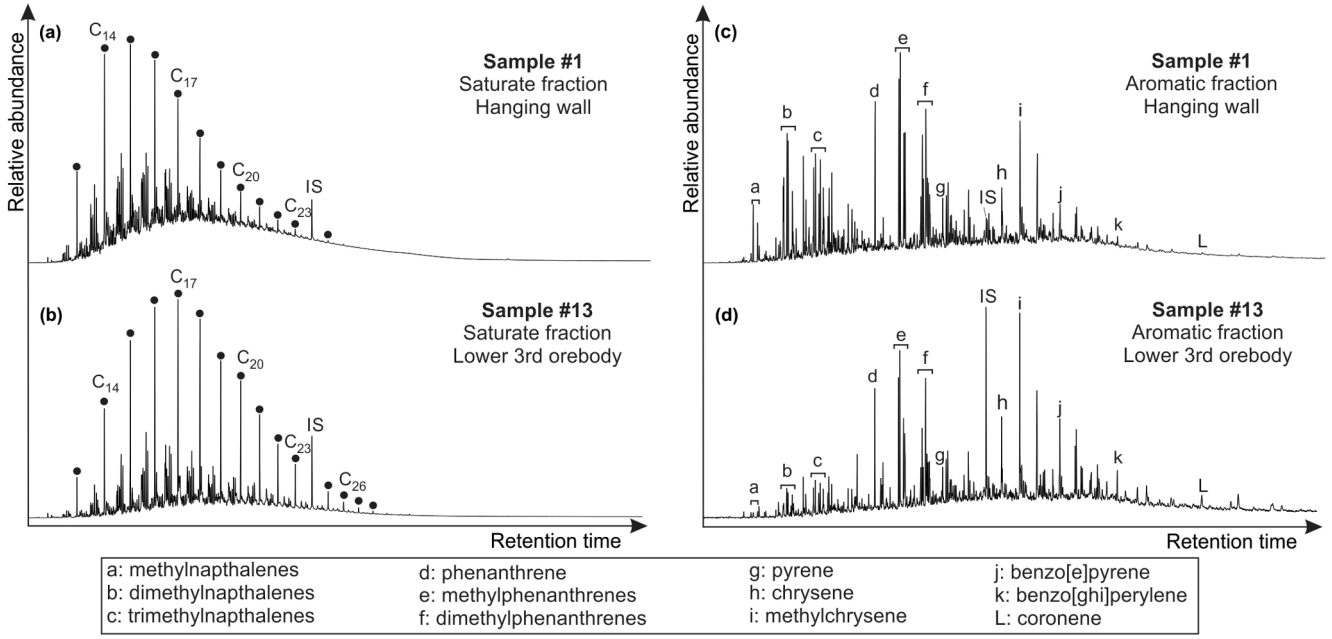

Fig. 2. Total ion chromatograms of saturate (a, b) and aromatic (c, d) hydrocarbon fractions from hanging wall (182.6 m above orebody) and lower 3rd orebody samples. Black circles represent *n*-alkanes. IS = internal standard.

Table 2
PAH concentrations in ppb relative to organic carbon mass.

Sequence	Sample ID	Drill core	Depth, (m)	Relative depth[a], (m)	P[b]	Pyrene	Chrysene	Benzo[e] pyrene	Benzo[ghi] perylene	Coronene
Hanging wall	#1	BS024-01	16.4	−182.6	18 432	3 733	9 136	4 462	1 315	142
	#2	BS024-01	41.5	−157.7	20 870	5 025	12 954	6 056	2 069	502
	#5	BS024-01	105.1	−94.1	4 290	1 522	3 263	2 761	983	215
	#6	BS024-01	146.1	−53.1	22 726	5 084	15 872	8 023	3 559	894
	#9	MRM 2012–03	157.8	−3.0	8 918	1 903	5 501	2 888	1 188	n.d.
Interore 7/8	#10	BS024-01	201.1	2.1	11 026	2 211	5 581	2 444	987	310
Orebody 6	#11	BS024-01	210.0	11.0	11 195	2 540	5 810	2 910	1 203	353
Interore 5/6	#12	BS024-01	215.7	16.7	16 145	4 223	6 568	3 147	1 840	583
Lower 3rd orebody	#13	MRM 2012–03	190.4	29.5	14 489	3 080	11 305	8 499	3 270	766
Interore 2/3	#14	MRM 2012–03	197.9	37.0	1 673	468	920	617	303	136
Foot wall	#15	MRM 2012–03	210.8	49.9	4 393	817	2 045	1 191	411	n.d.
Unmineralized BCF	#16	LV09	477	–	83 339	12 786	30 010	14 068	1 887	n.d.

[a] Depth in meters relative to the top of the ore body. [b]Phenanthrene.

analysed whole rock samples have poor to fair TOC contents varying between 0.2% and 0.7%. Only upper hanging wall samples #2 and #1 record good to very good organic richness with bulk TOC of 1.4% and 3% respectively. Bulk Tmax measurements for the majority of samples are unreliable due to low TOC and low S2 peak (S2 < 0.2). The two most reliable Tmax values, from hanging wall samples #2 and #1, indicate a late oil window maturity level.

To reduce the matrix effect on low-TOC samples, we also performed Rock-Eval measurements on kerogen concentrates. S2 peaks of kerogen concentrates were 1.3 to 37 times higher than for bulk rock measurements. Tmax values for the hanging wall fell into the range 440–448 °C, indicating maturities in the main oil window (Table 3, Fig. 3a). By contrast, and despite reasonably high carbon contents (0.7 to 7.7%), the kerogen concentrates from the underlying ore zone yielded inconsistently low Tmax values in the immature range from 386 to 424 °C, and one sample with low S2 peak (0.05) yielded 500 °C. Unreliable pyrograms (Supplementary Fig. 1a, b) indicate that the unrealistically low and high Tmax values in the ore zone are an artefact and do not represent the actual maturity of the kerogen concentrates.

4.3. Stable hydrogen and carbon isotopes

We measured the stable hydrogen isotopic composition (δ^2H) of *n*-alkanes from two ore zone samples and three hanging wall samples in

Table 3
Rock-Eval parameters for McArthur River samples.

Sequence	Sample ID	Bulk rock						Isolated kerogen					
		S1[a]	S2[b]	HI[c]	OI[d]	TOC[e] (%)	Tmax[f] (°C)	S1	S2	HI	OI	TOC (%)	Tmax (°C)
Hanging wall	#1	0.19	0.67	22	4	2.99	443	0.32	3.09	15	8	20.6	443
	#2	0.03	0.29	20	6	1.44	463	0.44	2.22	10	4	22.12	440
	#5	0.02	0.14	33	17	0.42	446*	0.91	2.85	30	6	9.58	440
	#6	0.01	0.03	9	34	0.32	467*	0.3	1.07	16	11	6.8	448
	#9	0.01	0.01	3	135	0.37	438*	0.1	0.41	21	7	1.98	442
Interore 7/8	#10	0.01	0.05	27	97	0.2	457*	0.24	0.64	8	8	7.74	424
Orebody 6	#11	0.01	0.1	22	52	0.48	441*	0.03	0.05	3	25	1.62	500*
Interore 5/6	#12	0	0.05	17	92	0.29	450*	0.05	0.21	11	5	1.87	422
Lower 3rd orebody	#13	0.03	0.1	20	32	0.52	413*	0.05	0.24	33	11	0.73	386
Interore 2/3	#14	0	0.04	7	59	0.68	442*	0.04	0.05	5	1	1.02	418*
Foot wall	#15	0.01	0.04	11	54	0.35	468*	0.78	1.49	10	2	14.2	436

[a] Free hydrocarbons, mg HC/g rock. [b]Generative potential, mg HC/g rock. [c]Hydrogen Index HI = S2*100/TOC, mg HC/g TOC. [d]Oxygen Index OI = S3*100/TOC, mg CO_2/g TOC. [e]Total Organic Carbon. [f]Temperature at maximum of S2 peak. * – low S2 (<0.2), Tmax is unreliable.

the McArthur River mine. Non-weighted average δ^2H of orebody *n*-alkanes *n*-C_{16} to *n*-C_{20} range from −78‰ to −82‰, whereas hanging wall *n*-alkanes range from −78‰ to −79‰ for samples #3 and #5 and reach −51‰ in sample #1 (Table 4). Fig. 4 illustrates the comparison of δ^2H values measured in the current study with previously published *n*-alkane values from the ore lens 5 (Williford et al., 2011) and an unmineralized Barney Creek Fm sample from LV09 drill core distal to the McArthur River deposit. Our measurements demonstrate that *n*-alkanes from the ore sequence and hanging wall are around 40‰ enriched in ^2H compared to *n*-alkanes from the unmineralized sample from the LV09 drill core (Fig. 4).

Stable carbon isotopes of Barney Creek Fm kerogen ($\delta^{13}C_{ker}$) only show slight variability, ranging from –32.8‰ to −34.0‰ (Table 4). The similarities between $\delta^{13}C_{ker}$ values in the orebody and unmineralized hanging wall and foot wall demonstrate that hydrothermal fluids did not significantly affect the isotopic composition of the orebody kerogen. Measurements of the stable carbon isotopic composition ($\delta^{13}C$) of *n*-alkanes are available for two samples from the ore zone, three from the hanging wall and one from the foot wall. Non-weighted average $\delta^{13}C$ of orebody *n*-alkanes *n*-C_{16} to *n*-C_{23} range from −29.3‰ to −30.8‰, whereas hanging wall and foot wall *n*-alkanes range from −25.0‰ to −29.5‰ (Table 4).

5. Discussion

5.1. Thermal maturity and origin of the bitumen

The solid black circles in Fig. 3a summarize previously published Rock-Eval data for the McArthur River deposit (Logan et al., 2001). While hanging wall samples indicate a normal burial maturity trend in the oil window (450–470 °C), the ore succession yields strongly elevated Tmax values (>520 °C). Fig. 3b illustrates organic matter reflectance measurements (random Ro) up to 2.4% in the orebody (Logan et al., 2001). At the same time, unmineralized layers within the ore zone have random Ro values that are consistent with burial maturities in the oil window (Fig. 3b) (Logan et al., 2001). These observations were used in support of an epigenetic model, where hot fluids percolated through permeable sedimentary layers forming the ore lenses but did not affect intercalated low permeability muddier beds (Logan et al., 2001). However, it seems questionable that inter-ore layers of millimetre to centimetre-scale could have escaped thermal alteration during ore genesis while hot brines flowed through the adjacent metal-rich layers. Additionally, since no information about S2 values is available for the published Rock-Eval data, and as the orebody is generally kerogen poor, the reliability of the Tmax values in the ore zone is uncertain.

In the current study, we obtained Rock-Eval data on kerogen concentrates uncompromised by possible mineral matrix effects and low TOC. Newly acquired Tmax values reconfirm oil window maturity in the hanging wall and also the foot wall. However, kerogen concentrates from the orebody yield unreliable pyrograms and/or low S2 values (Supplementary Fig. 1a, b). Tmax measurements obtained from these pyrograms are significantly below (386–424 °C) or above (500 °C) the oil window (Fig. 3a, Table 3) and do not indicate the actual maturity of the kerogen concentrates. Since the carbon content of the kerogen concentrates of the orebody samples is high enough to preclude detection limit problems, the low S2 peaks and unrealistic Tmax values must have a different explanation. We interpret the random variable Tmax values as an indicator for severely altered organic matter, likely related to locally elevated temperatures in the ore zone. Presence of pyrolytic kerogen in the orebody is in agreement with previous Rock-Eval and organic matter reflectance data from Logan et al. (2001) and high temperatures (~310 °C) estimated by Symons (2007) based on the orebody organic matter reflectance measurements of Crick (1992). Such temperatures are above the bacterial sulphate reduction range and are most consistent with thermochemical sulphate reduction.

Bitumen-based maturity parameters from our study are inconsistent with kerogen-based maturity data (Fig. 3). Rc(MPDF) values in the range 1.1 to 1.4% indicate normal burial maturities within the beginning of the gas window for the entire sediment package from the hanging wall, through the orebody and into the foot wall (Fig. 3c). Moreover, within the ore zone, maturities do not vary between mineralized and non-mineralized layers. The new and previous (e.g., Williford et al., 2011) bitumen Rc(MPDF) values contradict the Tmax and reflectance data from Logan et al. (2001) and Tmax from the current study that all suggest strongly elevated maturities in the ore zone (Fig. 3). The discrepancy between bitumen-based and kerogen-based parameters is best explained by a thermal anomaly during ore formation accompanied by alteration of the kerogen and destruction of indigenous hydrocarbons. The detected hydrocarbons in the orebody, which indicate normal burial maturities, must then represent migrated bitumen.

In order to obtain additional information about organic sources and geological processes in the McArthur River mine, we measured stable hydrogen (δ^2H) and carbon ($\delta^{13}C$) isotopic compositions of *n*-alkanes in orebody and hanging wall samples. Williford et al. (2011) demonstrated that McArthur River orebody *n*-alkanes are enriched in ^2H by up to 50–60‰ relative to *n*-alkanes in unmineralized Barney Creek Fm sediments from the GR-10 core distal from the mine. Williford et al. (2011) interpreted this as a result of equilibrium hydrogen exchange during ore genesis with a highly ^2H-enriched fluid, presumably coming from evaporites of the underlying Tawallah Group. However, due to limited sample availability, Williford et al. (2011) were not able to test this hypothesis by comparing the δ^2H composition of *n*-alkanes from the orebody with samples from the hanging wall. A strong δ^2H compositional difference of saturated hydrocarbons in the hanging wall and orebody would confirm the existence of isotopically heavy ore-forming brines ascending from the nearby fault system and exchanging hydrogen

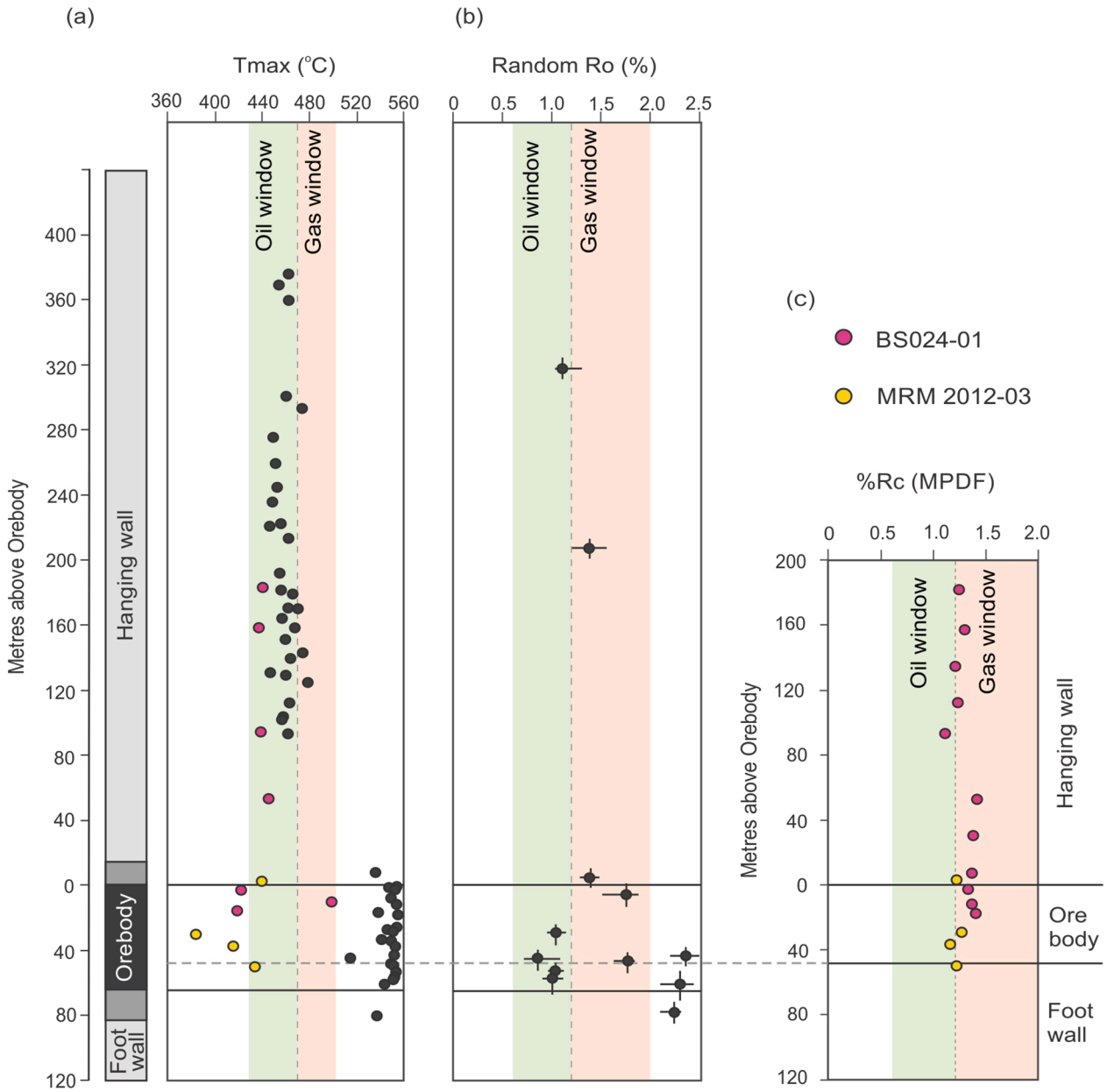

Fig. 3. Previous Tmax (a) and organic matter reflectance (b) data in black from drill hole and mine samples around McArthur River deposit, plotted relative to the orebody (modified from Logan et al., 2001); and Tmax data on isolated kerogen from the current study (pink and yellow circles). (c) Calculated vitrinite reflectance Rc(MPDF) for the extracted hydrocarbons from two McArthur River drill cores. Oil window: Rc between 0.6% and 1.2%, Tmax between 435 and 470 °C. Gas window: Rc between 1.2% and 2%, Tmax between 470 and 500 °C. (For interpretation of the references to colour in this figure legend, the reader is referred to the web version of this article.)

Table 4
Hydrogen and carbon isotope values for McArthur River samples.

Sequence	Sample ID	Internal sample ID	Relative depth[a], (m)	δ^2H alk[b](‰)	δ^{13}C ker[c] (‰)	δ^{13}C alk[d] (‰)
Hanging wall	#1	17G013	−182.6	−51	−33.4	−25.02
	#2	17G019	−157.7	n.d.	−34.0	−25.50
	#3	19G019	−135.6	−78	n.d.	n.d.
	#5	17G020	−94.1	−79	−33.3	−29.45
Lower 3rd orebody	#13	17G014	29.5	−78	−33.4	−29.34
Interore 2/3	#14	17G015	37.0	−82	−32.8	−30.76
Foot wall	#15	17G012	49.9	n.d.	−33.1	−26.18

[a] Depth in meters relative to the top of the ore body. [b]Stable hydrogen isotopic composition of *n*-alkanes (average of *n*-$C_{16–20}$). [c]Organic carbon isotope values of kerogen. [d]Stable carbon isotopic composition of *n*-alkanes (average of *n*-$C_{16–23}$). N.d. – not determined.

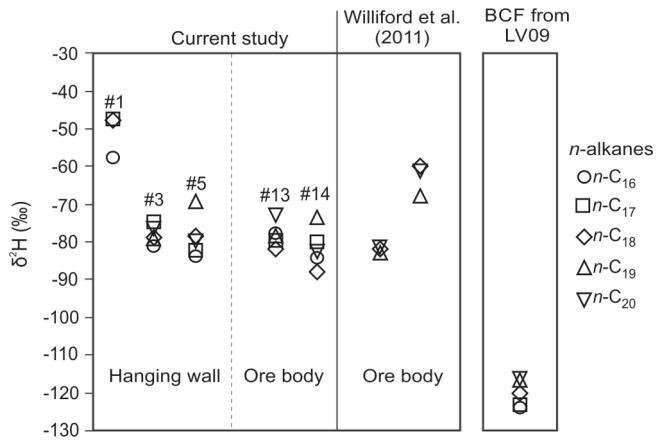

Fig. 4. Comparison of hydrogen isotope values (δ^2H) of *n*-alkanes from hanging wall and orebody samples from the current study, previously reported values from the ore lens 5 (samples 3 and 1; Williford et al., 2011) and a low maturity unmineralized Barney Creek Formation sample from LV09 drill core (485 m depth).

with McArthur River organic matter in the orebody. However, even though our measurements confirm that *n*-alkanes from the ore sequence are enriched in ^2H compared to immature and non-altered *n*-alkanes from the LV09 drill core, we detected similarly heavy isotopic compositions in the hanging wall above the ore (Fig. 4). This observation is more consistent with a general ^2H-enrichment of *n*-alkanes caused by kinetic fractionation effects at relatively high thermal maturities in the full McArthur River succession (e.g., Tang et al., 2005; Vinnichenko et al., 2021). Accordingly, heavy δ^2H values of *n*-alkanes in the orebody are not necessarily related to hydrogen exchange with evaporitic hydrothermal fluids, as was proposed by Williford et al. (2011). Instead, similar δ^2H values of orebody and hanging wall *n*-alkanes are consistent with the hypothesis that hydrocarbons in the ore zone migrated from surrounding unmineralized Barney Creek Fm sediments. Similarities in the distributions of saturated (Fig. 2a, b) and aromatic (Fig. 2c, d) fractions in the hanging wall and orebody also support this hypothesis.

The $\delta^{13}C$ composition of *n*-alkanes in the orebody is harder to explain. *n*-Alkanes in the orebody are depleted in ^{13}C relative to the hanging wall and foot wall *n*-alkanes by 1–5‰ (Table 4). A recent study by Vinnichenko et al. (2021) demonstrated a strong positive correlation between $\delta^{13}C$ of *n*-alkanes and thermal maturity in the unmineralized Barney Creek Fm (Fig. 5). Fig. 5 illustrates that $\delta^{13}C$ values of *n*-alkanes from the lower ore lens 3 and 2/3 inter-ore layer fall outside of this

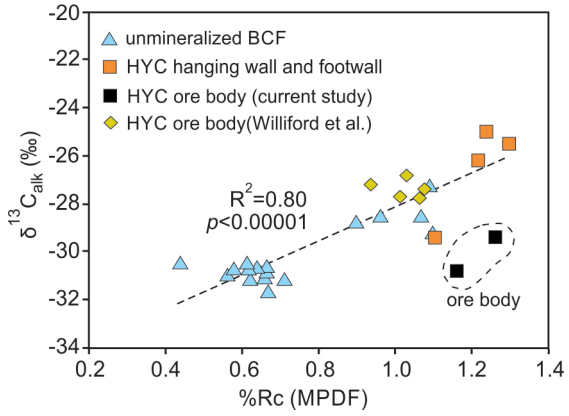

Fig. 5. Comparison of bitumens from McArthur River orebody and unmineralized Barney Creek Formation in a cross plot of $\delta^{13}C$ of *n*-alkanes (average of *n*-$C_{16–23}$) and calculated vitrinite reflectance Rc(MPDF) (Vinnichenko et al., 2021).

correlation, while values from the ore lens 5 measured by Williford et al. (2011) follow the expected trend. The data suggest that the McArthur River orebody contains more than one charge of migrated hydrocarbons that were expelled from their source rock at different stages of maturation and/or are from different stratigraphic levels. Moreover, it is possible that migrated hydrocarbons in the orebody have varied $\delta^{13}C$ values of *n*-alkanes due to different maturation mechanisms acting on in-situ bitumens and migrated oils. The complex isotope systematics of the McArthur River warrant further study.

We can draw two conclusions from the kerogen and bitumen maturity data. Firstly, organic matter in ore zone sediments suffered severe thermal alteration during the ore forming process and, secondly, the hydrocarbons in the orebody largely represent bitumens that migrated from surrounding sediments at a later stage. Therefore, the orebody hydrocarbons do not reflect the temperature and activity of the metal-bearing fluids.

5.2. *Polycyclic aromatic hydrocarbons (PAH) and temperature of the ore-forming fluid*

In support of an epigenetic model, a study by Chen et al. (2003) found distributions of PAH in the McArthur River ore zone similar to those seen in hydrothermal petroleum from the Guaymas Basin in the Gulf of California and north American Middle Valley (Kawka and Simoneit, 1990; Simoneit, 1994), proposing high formation temperatures of 250–400 °C. The authors observed that PAH concentrations decrease with distance from the source of the mineralizing fluids. This was explained by the theory that the PAH in the McArthur River were distributed laterally by ore-forming fluids through permeable layers in the sediment and precipitated during cooling of the fluids.

A follow-up study by Williford et al. (2011) suggested that a significant portion of PAH in the orebody likely originated in black shales of the underlying Tawallah Group at a depth of 6 km and temperatures of 250 °C and later migrated into the McArthur River deposit. The fluids containing PAH migrated along a flower structure associated with the Emu Fault and cooled to 200 ± 20 °C before reaching the Barney Creek Fm sediments. However, the temperature of 200 ± 20 °C was estimated based on reported Rc(MPI) values up to 1.6% for the ore lens 5. As described in section 4.1, Rc(MPI) in Williford et al. (2011) in fact range between 1.1 and 1.2%, which is also consistent with other maturity indices Rc(MPDF) = 0.9–1.1% and Rc(MPR) = 0.9–1.0%. Therefore, bitumen-based maturity parameters for the ore lens 5 correspond more to a temperature around 160 °C. Additionally, if the PAH formation temperatures of 250 °C proposed by Williford et al. (2011) are correct, then methyl-phenanthrene based indices (MPI, MPDF and MPR) should reflect higher maturity values consistent with such temperatures (Rc ~ 3–3.5% for T = 250 °C). However, this is contradicted by the lower maturity of the hydrocarbons found by Williford et al. (2011) and in the current study. Since orebody samples show the same bitumen maturity values as in the hanging wall and foot wall (Fig. 3c), we propose that PAH in the orebody migrated from a more proximal source than the Tawallah Group, possibly the Barney Creek Fm itself. According to Chen et al. (2003), some PAH are two to three times more abundant in ore relative to enclosing inter-ore layers (in ppb over TOC). We did not observe such PAH distributions in our sample set (Fig. 6, Table 2). However, it is possible that the PAH in the orebody observed by Chen et al. (2003) may represent a mixture between small amounts of syngenetic high-maturity PAH and PAH that migrated into the orebody during a later event from surrounding sediments.

In the current study, we detected similar distributions of PAH in the ore zone and in the hanging wall up to 180 m above the ore (Figs. 2, 6). Several interpretations could explain the presence of PAH in the hanging wall: (1) These molecules migrated into the hanging wall from other stratigraphic levels in the Barney Creek Fm; (2) the PAH are indigenous and formed at high temperatures due to continued influx of hydrothermal, base metal-poor but Fe-rich fluids into the hanging wall

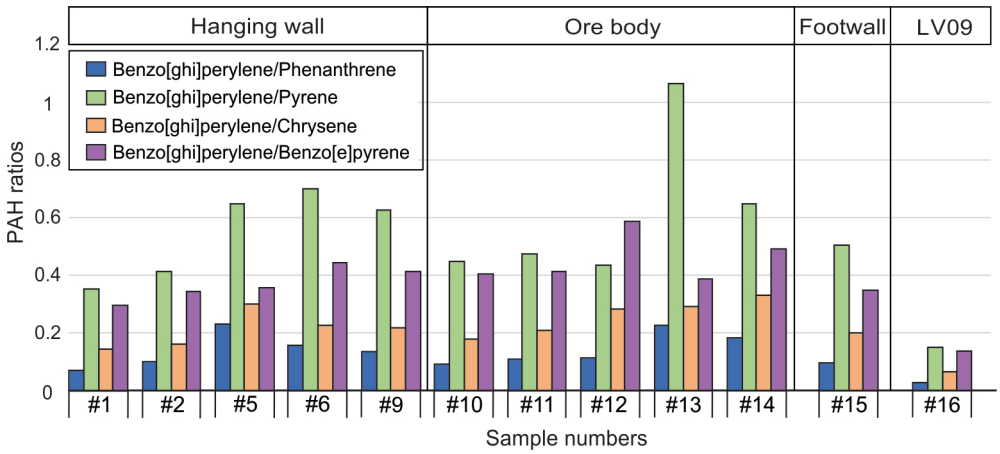

Fig. 6. Ratios of benzo[ghi]perylene to other PAH compounds in samples from McArthur River mine and immature unmineralized LV09 sample.

sediments after the cessation of ore formation; (3) the PAH are indigenous and formed through burial-temperature processes independent of hydrothermal fluids. To test the first hypothesis, we plotted the concentrations of individual PAH in hanging wall and foot wall bitumens against TOC (Fig. 7). The plot reveals significant linear correlations (R^2 = 0.88–0.95; n = 6), demonstrating that the PAH in the hanging wall are indigenous and that hypothesis (1) is false. If the second hypothesis is correct, then organic matter in the hanging wall should have experienced the same thermal alteration as organic matter in the orebody. However, this is not compatible with Tmax data that reveals a normal burial maturity trend in the hanging wall but highly elevated maturities in the ore zone (Fig. 3a). Hypothesis (3), suggesting a low-temperature origin of the PAH, is supported by the observation that low maturity Barney Creek Fm sediments from drill hole LV09 distal to the McArthur River mine contain even higher abundances of PAH (relative to TOC) than the McArthur River orebody (Table 2), including the same type of compounds and in broadly similar distributions despite considerable maturity differences (Fig. 6). It is thus clear that the PAH in the hanging wall are a component of the original bitumen that formed through burial-temperature processes, while the bulk of PAH in the orebody migrated from surrounding sediments. As a result, PAH distributions in the McArthur River mine cannot be used as indication for high temperatures (250–400 °C) of ore-forming fluids.

6. Conclusions

A comparison of kerogen and bitumens in the McArthur River orebody with the hanging and foot wall indicates that the original organic matter in the orebody was altered by pyrolytic temperatures and/or thermochemical sulphate reduction. However, the extractable hydrocarbons in the ore zone demonstrate much lower thermal maturities than the kerogen and must have migrated into the Zn-Pb deposit from surrounding sediments after mineralization. PAH found in the McArthur River orebody are also detected in similar amounts and distributions in the unmineralized hanging wall. Thus, the bulk of these compounds migrated into the orebody and formed through burial temperature processes and not during hydrothermal activity, as previously assumed. However, a small proportion of PAH in the ore might be an indigenous residue of hydrothermal processes.

As the hydrocarbons migrated into the orebody, they cannot provide information about the temperature of mineralizing fluids, negating evidence for temperatures of 250 to 400 °C (Chen et al., 2003) or 200 °C (Williford et al., 2011). Yet, new and previous Rock-Eval data and reflectance measurements indicate that the organic matter in the orebody was severely altered, including the ore lenses and inter-ore breccia. The data is most consistent with the activity of metal-bearing fluids with temperatures in the range of thermochemical sulphate reduction but inconsistent with bacterial sulphate reduction.

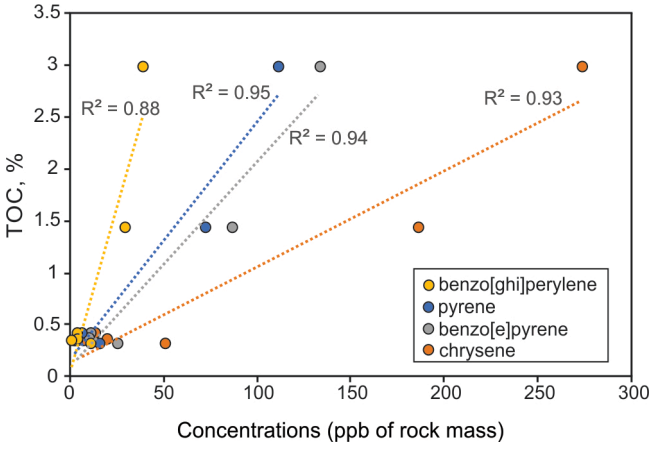

Fig. 7. Correlation of TOC with concentrations of various polycyclic aromatic hydrocarbons in hanging wall samples.

Declaration of Competing Interest

The authors declare that they have no known competing financial interests or personal relationships that could have appeared to influence the work reported in this paper.

Acknowledgements

We are grateful to Jacob Sohn and Junhong Chen for technical assistance with isotope measurements and Ian Long for isolation of kerogen in the Organic Geochemistry laboratory at Geoscience Australia. We thank Ruslan Khamidullin (Lomonosov MSU) for help with Rock-Eval analysis. We thank Darryl Stacey from the Darwin Core Library (NTGS) for access to McArthur Basin drill cores. JJB and NW thank McArthur River Mining Pty Ltd for their support of this study and, in particular, Christopher Hy and Ed Morris for facilitating sample collection. We are grateful to two anonymous reviewers and Marcus Kunzmann for their helpful comments. This research was financially supported by Australian Research Council grants DP160100607 and DP170100556 (to JJB). GV acknowledges support from an Australian Government Research Training Program (RTP) Scholarship. AJMJ publishes with permission of the CEO, Geoscience Australia. The authors declare no conflicting interests, financial or otherwise.

Appendix A. Supplementary data

Supplementary data to this article can be found online at https://doi.org/10.1016/j.oregeorev.2021.104129.

References

Ahmad, M., Dunster, J.N. and Munson, T.J., 2013. Chapter 15: McArthur Basin: in Ahmad M and Munson TJ (compilers).'. Geology and mineral resources of the Northern Territory'. Northern Territory Geological Survey, Special Publication, 5.

Baskin, D.K., 1997. Atomic H/C ratio of kerogen as an estimate of thermal maturity and organic matter conversion. AAPG Bull. 81 (9), 1437–1450.

Blaikie, T., Kunzmann, M., 2020. Geophysical interpretation and tectonic synthesis of the Proterozoic southern McArthur Basin, northern Australia. Precambr. Res. 343, 105728.

Boreham, C., Crick, I., Powell, T., 1988. Alternative calibration of the Methylphenanthrene Index against vitrinite reflectance: Application to maturity measurements on oils and sediments. Org Geochem. 12 (3), 289–294.

Brocks, J.J., Buick, R., Logan, G.A., Summons, R.E., 2003. Composition and syngeneity of molecular fossils from the 2.78 to 2.45 billion-year-old Mount Bruce Supergroup, Pilbara Craton, Western Australia. Geochim. Cosmochim. Acta 67 (22), 4289–4319.

Brocks, J.J., Grosjean, E., Logan, G.A., 2008. Assessing biomarker syngeneity using branched alkanes with quaternary carbon (BAQCs) and other plastic contaminants. Geochim. Cosmochim. Acta 72 (3), 871–888.

Brocks, J.J., Love, G.D., Summons, R.E., Knoll, A.H., Logan, G.A., Bowden, S.A., 2005. Biomarker evidence for green and purple sulphur bacteria in a stratified Palaeoproterozoic sea. Nature 437, 866.

Brocks, J.J., Schaeffer, P., 2008. Okenane, a biomarker for purple sulfur bacteria (Chromatiaceae), and other new carotenoid derivatives from the 1640Ma Barney Creek Formation. Geochim. Cosmochim. Acta 72 (5), 1396–1414.

Bull, S., 1998. Sedimentology of the Palaeoproterozoic Barney Creek formation in DDH BMR McArthur 2, southern McArthur basin, northern territory. Aust. J. Earth Sci. 45 (1), 21–31.

Chen, J., Fu, J., Sheng, G., Liu, D., Zhang, J., 1996. Diamondoid hydrocarbon ratios: novel maturity indices for highly mature crude oils. Org Geochem. 25 (3–4), 179–190.

Chen, J., Walter, M.R., Logan, G.A., Hinman, M.C., Summons, R.E., 2003. The Paleoproterozoic McArthur River (HYC) Pb/Zn/Ag deposit of northern Australia: organic geochemistry and ore genesis. Earth Planet. Sci. Lett. 210 (3–4), 467–479.

Crick, I.H., 1992. Petrological and maturation characteristics of organic matter from the Middle Proterozoic McArthur Basin. Australia. Australian Journal of Earth Sciences 39 (4), 501–519.

Eldridge, C., Williams, N., Walshe, J.L., 1993. Sulfur isotope variability in sediment-hosted massive sulfide deposits as determined using the ion microprobe SHRIMP; II, A study of the HYC Deposit at McArthur River, Northern Territory. Australia. Economic Geology 88 (1), 1–26.

Greenwood, P.F., Brocks, J.J., Grice, K., Schwark, L., Jaraula, C.M.B., Dick, J.M., Evans, K.A., 2013. Organic geochemistry and mineralogy. I. Characterisation of organic matter associated with metal deposits. Ore Geol. Rev. 50, 1–27.

Ireland, T., Large, R.R., McGoldrick, P., Blake, M., 2004. Spatial distribution patterns of sulfur isotopes, nodular carbonate, and ore textures in the McArthur River (HYC) Zn-Pb-Ag deposit, Northern Territory. Australia. Economic Geology 99 (8), 1687–1709.

Jackson, M., Muir, M.D. and Plumb, K.A., 1987. Geology of the southern McArthur Basin, Northern Territory, 220. Australian Government Publishing Service.

Jarrett, A., Cox, G., Southby, C., Hong, Z., Palatty, P., Carr, L. and Henson, P., 2018. Source rock geochemistry of the McArthur Basin, northern Australia: Rock-Eval pyrolysis data release. Record 2018/024. Geoscience Australia, Canberra.

Jarrett, A.J.M., Schinteie, R., Hope, J.M., Brocks, J.J., 2013. Micro-ablation, a new technique to remove drilling fluids and other contaminants from fragmented and fissile rock material. Org Geochem. 61, 57–65.

Kawka, O.E., Simoneit, B.R., 1990. Polycyclic aromatic hydrocarbons in hydrothermal petroleums from the Guaymas Basin spreading center. Appl. Geochem. 5 (1–2), 17–27.

Kunzmann, M., Schmid, S., Blaikie, T.N., Halverson, G.P., 2019. Facies analysis, sequence stratigraphy, and carbon isotope chemostratigraphy of a classic Zn-Pb host succession: The Proterozoic middle McArthur Group, McArthur Basin, Australia. Ore Geol. Rev. 106, 150–175.

Kvalheim, O.M., Christy, A.A., Telnæs, N., Bjørseth, A., 1987. Maturity determination of organic matter in coals using the methylphenanthrene distribution. Geochim. Cosmochim. Acta 51 (7), 1883–1888.

Large, R., Bull, S., Selley, D., Yang, J., Cooke, D., Garven, G., McGoldrick, P., 2002. Controls on the formation of giant stratiform sediment-hosted Zn-Pb-Ag deposits: with particular reference to the north Australian Proterozoic. University of Tasmania, Centre for Special Ore Deposit and Exploration (CODES) Studies. Publication 4, 107–149.

Large, R.R., Bull, S.W., Cooke, D.R., McGoldrick, P.J., 1998. A genetic model for the HYC Deposit, Australia; based on regional sedimentology, geochemistry, and sulfide-sediment relationships. Econ. Geol. 93 (8), 1345–1368.

Large, R.R., Bull, S.W., Winefield, P.R., 2001. Carbon and oxygen isotope halo in carbonates related to the McArthur River (HYC) Zn-Pb-Ag deposit, north Australia: Implications for sedimentation, ore genesis, and mineral exploration. Econ. Geol. 96 (7), 1567–1593.

Logan, G.A., Hinman, M.C., Walter, M.R., Summons, R.E., 2001. Biogeochemistry of the 1640 Ma McArthur River (HYC) lead-zinc ore and host sediments, Northern Territory. Australia. Geochimica et Cosmochimica Acta 65 (14), 2317–2336.

Magnall, J.M., Gleeson, S., Hayward, N., Rocholl, A., 2020. Massive sulfide Zn deposits in the Proterozoic did not require euxinia. Geochemical Perspectives Letters 13, 19–24.

McGoldrick, P., Winefield, P., Bull, S., Selley, D., Scott, R., 2010. Sequences, synsedimentary structures, and sub-basins: the where and when of SEDEX zinc systems in the southern McArthur Basin. Australia. Soc. Econ. Geol. Spec. Publ 15, 1–23.

Munson, T., 2014. Petroleum geology and potential of the onshore Northern Territory, 2014. Northern Territory Geological Survey.

Oehler, J.H., 1977. Microflora of the HYC pyritic shale member of the Barney Creek Formation (McArthur Group), middle Proterozoic of northern Australia. Alcheringa 1 (3), 315–349.

Page, R.W., Sweet, I.P., 1998. Geochronology of basin phases in the western Mt Isa Inlier, and correlation with the McArthur Basin. Aust. J. Earth Sci. 45 (2), 219–232.

Pawlowska, M.M., Butterfield, N.J., Brocks, J.J., 2013. Lipid taphonomy in the Proterozoic and the effect of microbial mats on biomarker preservation. Geology 41 (2), 103–106.

Radke, M., 1988. Application of aromatic compounds as maturity indicators in source rocks and crude oils. Mar. Pet. Geol. 5 (3), 224–236.

Radke, M., Welte, D.H., 1983. The methylphenanthrene index (MPI): a maturity parameter based on aromatic hydrocarbons. Advances Organic Geochemistry 1981, 504–512.

Simoneit, B.R., 1994. Lipid/bitumen maturation by hydrothermal activity in sediments of Middle Valley, Leg 139.

Spinks, S.C., Pearce, M.A., Liu, W., Kunzmann, M., Ryan, C.G., Moorhead, G.F., Kirkham, R., Blaikie, T., Sheldon, H.A., Schaubs, P.M., 2020. Carbonate Replacement as the Principal Ore Formation Process in the Proterozoic McArthur River (HYC) Sediment-Hosted Zn-Pb Deposit, Australia. Econ. Geol.

Summons, R.E., Powell, T.G. and Boreham, C.J., 1988. Petroleum geology and geochemistry of the Middle Proterozoic McArthur Basin, Northern Australia: III. Composition of extractable hydrocarbons. Geochimica et Cosmochimica Acta, 52(7): 1747-1763.

Symons, D., 2007. Paleomagnetism of the HYC Zn-Pb SEDEX Deposit, Australia: evidence of an epigenetic origin. Econ. Geol. 102 (7), 1295–1310.

Tang, Y., Huang, Y., Ellis, G.S., Wang, Y., Kralert, P.G., Gillaizeau, B., Ma, Q., Hwang, R., 2005. A kinetic model for thermally induced hydrogen and carbon isotope fractionation of individual n-alkanes in crude oil. Geochim. Cosmochim. Acta 69 (18), 4505–4520.

Vinnichenko, G., Jarrett, A.J., van Maldegem, L.M., Brocks, J.J., 2021. Substantial maturity influence on carbon and hydrogen isotopic composition of n-alkanes in sedimentary rocks. Org Geochem. 152, 104171.

Vinnichenko, G., Jarrett, A.J.M., Hope, J.M., Brocks, J.J., 2020. Discovery of the oldest known biomarkers provides evidence for phototrophic bacteria in the 1.73 Ga Wollogorang Formation. Australia. Geobiology 18 (5), 544–559.

Williford, K.H., Grice, K., Logan, G.A., Chen, J., Huston, D., 2011. The molecular and isotopic effects of hydrothermal alteration of organic matter in the Paleoproterozoic McArthur River Pb/Zn/Ag ore deposit. Earth Planet. Sci. Lett. 301 (1–2), 382–392.